Phenomenological classification of metals based on resistivity

Qikai Guo, César Magén, Marcelo J Rozenberg, Beatriz Noheda

Phenomenological classification of metals based on resistivity

Qikai Guo [1,2,*] César Magén [3,4] Marcelo J. Rozenberg [5] and Beatriz Noheda [1,6,†]

[1] *Zernike Institute for Advanced Materials, University of Groningen, 9747AG Groningen, The Netherlands*
[2] *School of Microelectronics, Shandong University, Jinan 250100, China*
[3] *Instituto de Nanociencia y Materiales de Aragón (INMA), CSIC-Universidad de Zaragoza, 50009 Zaragoza, Spain*
[4] *Laboratorio de Microscopías Avanzadas (LMA), Universidad de Zaragoza, 50018 Zaragoza, Spain*
[5] *Université Paris-Saclay, CNRS, Laboratoire de Physique des Solides, 91405 Orsay, France*
[6] *CogniGron Center, University of Groningen, 9747AG Groningen, The Netherlands*

(Received 14 October 2021; revised 7 August 2022; accepted 12 August 2022; published 29 August 2022)

Efforts to understand metallic behavior have led to important concepts such as those of strange metals, bad metals, or Planckian metals. However, a unified description of metallic resistivity is still missing. An empirical analysis of a large variety of metals shows that the parallel resistor formalism used in the cuprates, which includes T-linear and T-quadratic dependence of the electron scattering rates, can be used to provide a phenomenological description of the electrical resistivity in all metals, where these two contributions are shown to correspond to the first two terms of a Taylor expansion of the resistivity, detached from their physics origin, and thus valid for any metal. Here, we show that the different metallic classes are then determined by the relative magnitude of these two components and the magnitude of the extrapolated residual resistivity. These two parameters allow us to categorize a few systems that are notoriously hard to ascribe to one of the currently accepted metallic classes. This approach also reveals that the T-linear term has a common origin in all cases, strengthening the arguments that propose the universal character of the Planckian dissipation bound.

DOI: 10.1103/PhysRevB.106.085141

I. INTRODUCTION

Interactions of electrons with other (quasi)particles (e.g., phonons, magnons, or electrons themselves) are responsible for the electrical transport of metallic systems. In simple metals, electron-electron interactions lead to a Fermi-liquid description [1] of the resistivity at low temperatures (T) as a T^2 dependence, while a linear increase of resistivity is usually observed at high T because of the boosted scattering strength between electrons and phonons. However, this well-defined regime is met with problems in strongly correlated metals. This can happen when the metallic system is driven close to a quantum critical point, which gives rise to a T dependence of resistivity of the type T^n, with $1 \leqslant n < 2$ at low T [2,3]. Among those, the "strange metals," such as the optimally doped cuprates, present a puzzling linear-T dependence of resistivity that can range from very low T (thus discarding phonon scattering) to high T.

Deviations from the standard behavior also take place at high temperatures, when the increased scattering drives the mean free path (ℓ) to approach the Mott-Ioffe-Regel (MIR) limit [4,5], which compels the resistivity to show saturation at high T [6]. However, in some so-called incoherent or "bad metals," the resistivity overcomes this upper limit, implying such large scattering rates that, according to Heisenberg's principle, the uncertainty in the quasiparticle energy prevents their coherence, thus disqualifying the quasiparticle description altogether [7,8].

Different conduction mechanisms become dominant at different temperatures and thus an overall description of metallic resistivity over a wide temperature range requires considering the combined effect of the various contributions in a phenomenological manner. T-linear resistivity has been typically associated with electron-phonon scattering and thus such dependence was not expected at low temperatures. However, it is now well established that T-linear resistivity can emerge well below the Debye temperature in various systems, from simple metals to strongly correlated metals, as long as the scattering rate ($1/\tau$) per degrees Kelvin of the charge carriers reaches a universal bound, $k_B/\hbar$. This so-called *Planckian* dissipation limit (PDL) is independent of the distinct behavior and conduction mechanism [9]. These findings challenge the significance of a specific scattering mechanism in determining "strange" metallic transport and motivates the search for a phenomenological description that applies to a large variety of metals. In this paper we propose such a description.

II. RESULTS AND DISCUSSION

In Fig. 1(a), the $\rho(T)$ curves of a wide diversity of metallic systems are plotted together. These systems include cuprates with different doping levels, ruthenates, heavy fermions, alkali-doped C_{60}, iron pnictides, transition metals, and monovalent metals. These materials have been classified as simple metals, correlated metals, strange metals, bad metals, or Planckian metals. Compared with the slowly increasing

*Corresponding author: qikaiguo@sdu.edu.cn
†Corresponding author: b.noheda@rug.nl

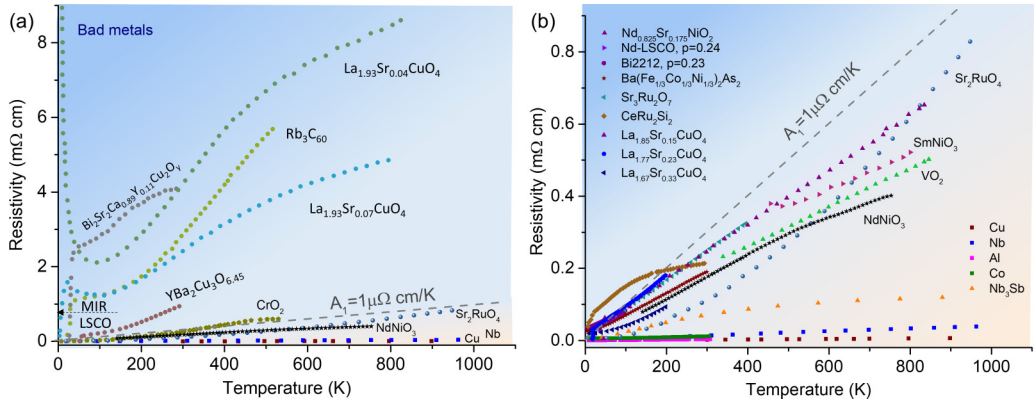

FIG. 1. Resistivity of various metallic systems. (a) Compilation plot showing the resistivity of various metallic systems. (b) Blow-up of the intermediate region in (a). The dashed line indicates the linear-T-resistivity slope of 1 $\mu\Omega$ cm; the arrow shows the MIR limit (0.7 mΩ cm) of $La_{2-x}Sr_xCuO_4$. [Data source: Cu, Nb [6,10–12]; Al, Co, and Pd [13]; Pb [14]; $La_{2-x}Sr_xCuO_4$ with $x = 0.17$–0.33 [15], with $x = 0.04$ and 0.07 [16,17]; $Bi_2Sr_2Ca_{0.89}Y_{0.11}Cu_2O_y$ [18]; Rb_3C_{60} [19,20]; $YBa_2Cu_3O_{6.45}$ [21]; Sr_2RuO_4 [22]; $CeRu_2Si_2$ [23,24]; CrO_2 [25–28]; VO_2 [29]; Nb_3Sb [30]; $SmNiO_3$ [31]; $Nd_{0.825}Sr_{0.175}NiO_2$ [32]; Nd-LSCO ($p = 0.24$) and Bi2212 ($p = 0.23$) [33]; $Ba(Fe_{1/3}Co_{1/3}Ni_{1/3})_2As_2$ [34]; $Sr_3Ru_2O_7$ [9].]

resistivity of simple metals (in the yellow region), for the metals displayed in the blue region, the slope of $\rho(T)$ at around 300 K (which in most cases is the maximum slope) is large, as expected from strong electron scattering. Among them, the underdoped cuprates and Rb_3C_{60} are well-established bad metals [6]. The resistivity in these systems can cross the ρ_{MIR} limit at relatively low temperatures and approach a value far beyond it at high temperatures, violating the quasiparticle scenario.

Notably, most correlated metals are located in an intermediate region between the good metals and the bad metals, as shown with more detail in the blow-up plot of Fig. 1(b). Interestingly, a number of these intermediate systems remain unclassified, such as Sr_2RuO_4 [22] and CrO_2 [25], which have been reported to possess properties of both conventional and bad metals. Other systems, such as $Sr_3Ru_2O_7$, $La_{1.6-x}Nd_{0.4}Sr_xCuO_4$ (Nd-LSCO) for hole doping $x \approx p = 0.24$, $Bi_2Sr_2CaCu_2O_8 + \delta$ (Bi2212) for hole doping $x \approx p = 0.23$, and $Ba(Fe_{1/3}Co_{1/3}Ni_{1/3})_2As_2$, have been discussed as Planckian metals [9,33,34]. However, regardless of their different origin and classification, the resistivity of all the metallic systems in the intermediate region show many comparable features. For instance, the maximum slope of resistivity in most of the materials is well below an upper limit of 1 $\mu\Omega$ cm/K. The same limit has been reported in high-T_c cuprates and was associated with the momentum-averaged scattering rate ($\hbar/\tau \sim \pi k_B T$) [35], which corresponds to the PDL. As mentioned earlier, the PDL concept has been put forward as the common origin of the linear-T resistivity in systems with very different scattering mechanisms, including high-T_c superconductors, other electron-correlated systems, and even simple metals [9].

In an effort to unify the behavior of the different metallic systems, we follow the seminal work of Hussey *et al.* in high-T_c cuprates [15], which shows that the resistivity of $La_{2-x}Sr_xCuO_4$ at various doping levels can be successfully described by a parallel resistor formalism [36] as

$$\rho(T)^{-1} = \rho_{ideal}(T)^{-1} + \rho_{sat}^{-1}, \quad (1)$$

where ρ_{ideal} is the resistivity in the absence of saturation, which is shunted by the large value of ρ_{sat} at high temperatures. An adequate definition of ρ_{ideal} is then needed in order to describe $\rho(T)$ in a wide temperature range. Based on a large body of experimental data, a dual-component model, with linear and quadratic terms, has been used in the cuprates [15,37] as

$$\rho_{ideal}(T) = \rho_0 + A_1 T + A_2 T^2, \quad (2)$$

where ρ_0 represents the residual resistivity, and the other two terms reflect the temperature dependence of the scattering rate with an isotropic T-quadratic component (assigned to electron-electron scattering) and an anisotropic T-linear component that is consistent with the PDL [15]. Generalizing this to other types of metals, A_1 and A_2 cannot be assigned to a specific scattering mechanism and the previous equation should be generally considered as a Taylor expansion of $\rho(T)$.

Here, we show that this dual-component parallel-resistor formalism (DC-PRF) can describe the metallic behavior of very distinct systems, independently of the dominant scattering mechanism. The DC-PRF has been used to fit the remarkable variety of resistivity data shown in Fig. 1, from the bad metals to the good metals. As shown in Figs. 2(a)–2(c) and the Supplemental Material [38], the electrical resistivity of all these materials can be well described by Eqs. (1) and (2). In all cases $A_2 < A_1$, reflecting a strong linear component at low temperatures (see Fig. S34 [38]). This analysis provides us with a unified view of metallic behavior. As shown in Figs. 3(a) and 3(b), the fitting of resistivity to all those metallic systems reveals a clear evolution of A_1 and A_2 as a function of their room-temperature resistivity ($\rho_{300\,K}$). Interestingly, the data include $NdNiO_3$ (NNO), which we consider in the present work as both a test case and an illustration of the utility of the formalism. In fact, this compound is attracting significant attention, since superconductivity was reported in the related infinite-layer system $Nd_{1-x}Sr_xNiO_2$ [39], and is a remarkable example of a material whose metallic behavior has been particularly difficult to classify [31,40,41]. For the present study, we have used epitaxial NNO films grown on

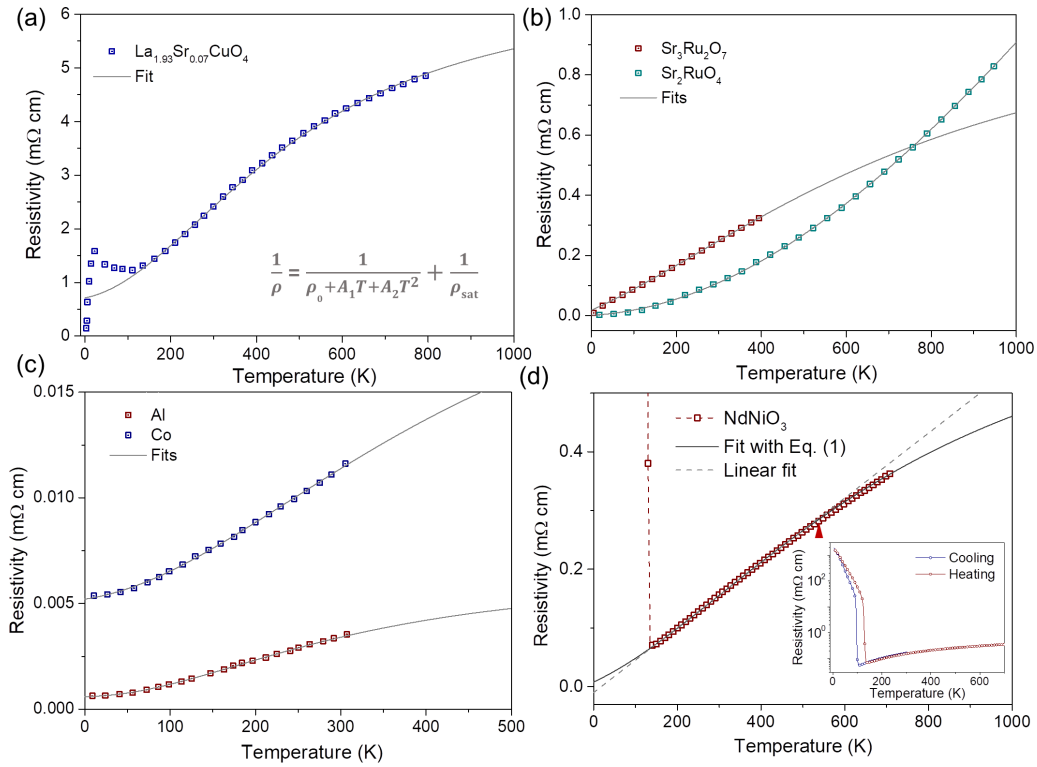

FIG. 2. Fitting of the electrical resistivity of various metallic systems using Eq. (1). (a) Underdoped cuprate. (b) Ruthenates. (c) Simple metals. (d) Nickelate ($NdNiO_3$). The triangle in (d) indicates the temperature above which the data deviate from a T-linear dependence. (Data sources: The resistivity of $NdNiO_3$ is measured in the present work, while the data of other systems are extracted from Refs. [9,13,16,22], respectively.)

$LaAlO_3$ substrates, which have been characterized in detail in our previous work [42,43]. The high-angle annular dark field (HAADF) scanning tunneling electron microscopy (STEM) image shown in Supplemental Material Sec. 1 demonstrates the high crystalline quality of the NNO films with an atomically sharp interface with the substrate [38]. In this 10-nm film, a first-order metal-to-insulator transition occurs below 150 K. Here, measurements of resistivity in an extended temperature range allow for a clear determination of the T dependence in the metallic state.

As shown in Fig. 2(d), a linear-T resistivity is observed in NNO in an ultrawide temperature range (about 400 K). In our previous works, we showed that this T-linear behavior can be achieved in optimized NNO films with low epitaxial strain and low defect content [42] and, more interestingly, it has signatures of Planckian dissipation [43]. With a further increase of T, the rise of $\rho(T)$ shows an obvious deviation from the linear dependence, which is caused by the addition of a parallel saturation resistance that takes over the behavior in the high-temperature regime [6,7,36]. Moreover, as in $NdNiO_3$ strong electron-electron interactions are expected, the combined effect of all these contributions should be considered. Indeed, we can show that the metallic resistivity of the $NdNiO_3$ film over a temperature range of 600 K can be well fit with the DC-PRF of Eqs. (1) and (2) with A_2 being more than two orders of magnitude smaller than A_1 (see Fig. S27 in the Supplemental Material [38]).

One of the interesting features unveiled in Fig. 3 is that the increase of A_1 saturates at a maximum value $\sim 1\ \mu\Omega$ cm/K, which we have previously discussed in relation to the definition of the intermediate region of Fig. 1(a). However, the DC-PRF allows us to extract the linear contribution to resistivity in a wider variety of metallic systems and in a wider temperature range. In this way, we find that the upper limit is actually obeyed by all the correlated systems, even in those well-established bad metals.

The same $A_1 \sim 1\ \mu\Omega$ cm/K limit has been reported in high-T_c cuprates [35] and has been associated with the PDL. Indeed, we notice that the extracted A_1 from those strange metals (inside the yellow-encircled region) approximately approaches this upper limit. Despite being derived for simple and isotropic Fermi surfaces, one can use the Drude formula of conduction to estimate the universal Planckian bound on dissipation ($1/\tau = k_B T/\hbar$) and obtain that $A_1 = (m^*/n)(k_B/e^2\hbar)$, which includes the carrier density (n) and carrier effective mass (m^*). This bound is therefore system specific and explains that normal metals, due to their lower m^*/n ratio [see Fig. 3(c) and Supplemental Material Sec. 3 [38]], display smaller A_1 values than the correlated metals. Indeed, as shown in the inset of Fig. 3(c), the product $A_1 n/m^*$, which characterizes the PDL, confirms that such a limit is generally obeyed [9]. Thus, our analysis shows that the Planckian bound is a significant contribution to the $\rho(T)$ in all investigated metals. The relevance of this limit also in systems that show nonlinear-T resistivity [44] is then clearly demonstrated using this approach.

In contrast, the quadratic A_2 coefficient does not display a bound and continues increasing to reach the largest values in

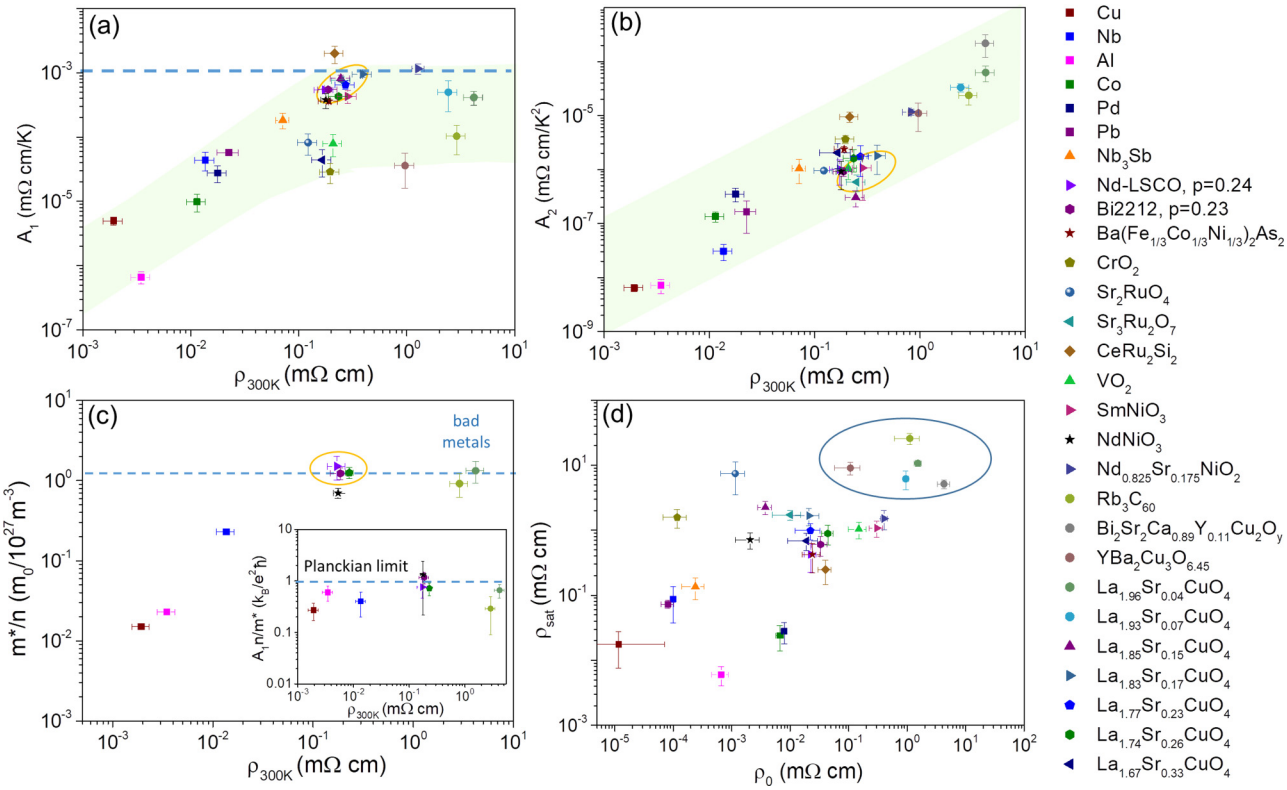

FIG. 3. Observed trends in the DC-PRF coefficients. From the fit of $\rho(T)$ in various metals to the DC-PRF model of Eqs. (1) and (2), the coefficients (a) A_1 and (b) A_2 are obtained and plotted as a function of the corresponding room-temperature resistivity ($\rho_{300\,\mathrm{K}}$). The blue dashed line in (a) indicates the maximum value obtained for $A_1 \sim 1\ \mu\Omega$ cm/K. Error bars are also obtained from the fitting results. Encircled in yellow are the strange metals. Shadows are a guide to the eye showing the general evolution of the coefficients. (c) The m^*/n ratio is plotted as a function of $\rho_{300\,\mathrm{K}}$, showing a trend similar to A_1. In the inset, $A_1 n/m^*$ is shown to remain at, or slightly below, $k_B/(e^2\hbar)$, which corresponds to the Planckian dissipation limit (PDL), also for the normal metals and bad metals. (d) Saturation resistivity (ρ_{sat}) as a function of residual resistivity (ρ_0). Encircled in blue are the bad metals.

bad metals [see Fig. 3(b)]. Even though A_2 cannot be associated with a unique physical process through all the metal classes, its magnitude reflects the strength of the electron scattering, with the smallest A_2 for the normal metals and the largest for the bad metals, as expected. Interestingly, in most of the investigated bad metals, ρ_0 (obtained from the DC-PRF fits) is also significantly larger than in other metals [see Fig. 3(d)], confirming the widespread notion that bad metals are dirty metals [45]. This fact, and the large A_2 values, are responsible for the increased ρ_{sat} values that characterize bad metals. Despite the large uncertainties associated with the values of ρ_{sat} [46], the results of the fits in the systems known as bad metals give rise to ultralarge values of ρ_{sat}, well above what has been generally considered to be their MIR limit (<1 mΩ cm [6,7]), as expected in this class of metals.

However, it is worth pointing out, first, that the role of the saturation term in the DC-PRF expression is in some cases (i.e., normal metals) that of linearizing the parabolic increase in resistance that arises from Eq. (2), in order to reproduce the linear electron-phonon regime at intermediate temperatures, while in some other cases, where the data show signs of saturation, this term can be directly associated with the MIR limit. This further emphasizes the phenomenological character of the DC-PRF expression. Second, the exact magnitude of the MIR limit for electron correlated metals is difficult to determine and it has been proposed that the small Fermi surfaces of these materials can lead to MIR values much larger than the ones earlier proposed [47].

Thus, our analysis shows that the different behavior of $\rho(T)$ in various systems is mainly determined by the relative importance of A_1 and A_2, which can be assessed by the magnitude of $T^* = A_1/A_2$, that is, the temperature at which the linear and quadratic terms in $\rho(T)$ become equal [48], and their ρ_0. Figure 4(a) shows ρ_0 as a function of T^*, evidencing that the bad metals show the smallest values of T^*, while the strange metals show the largest T^*. Indeed, the strange metals have a significantly smaller A_2, compared to bad metals, and similar A_1, which leads to a strongly decreased quadratic contribution, as expected from their close to linear dependence in an extended temperature range. Ayres *et al.* [49] proposed that the strange metals host two charge sectors, one containing coherent quasiparticles, and the other one containing scale-invariant "Planckian" dissipators [49]. This is well consistent with our findings, with $T^* = A_1/A_2$ representing the temperature at which one sector takes over the other one.

According to Fig. 4, there are metals with low ρ_0 ($<10^{-3}$ mΩ cm), intermediate ρ_0 ($\sim 10^{-2}$ mΩ cm), and large ρ_0 (~ 1 mΩ cm), and they can have low T^* (< 30 K), intermediate T^* (30 K $< T^* <$ 300 K), or large T^* (> 300 K). Good metals are characterized by a low ρ_0, while bad metals are

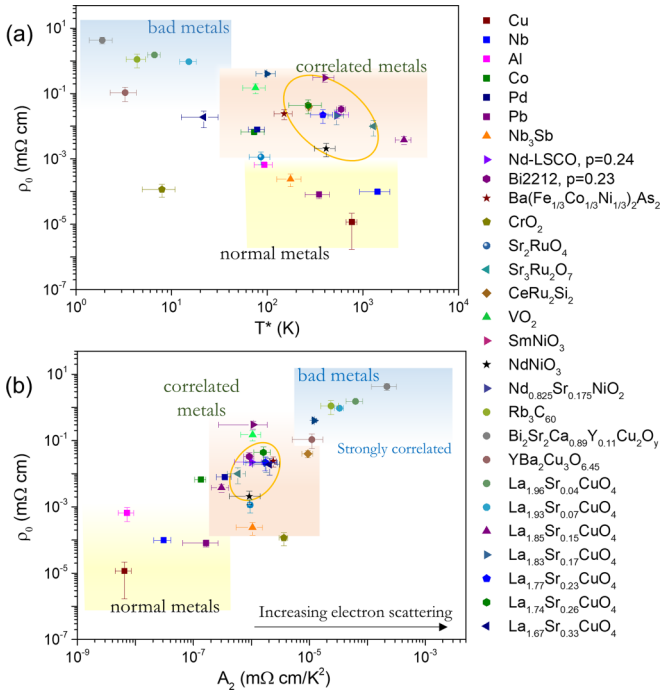

FIG. 4. Key parameters for the general classification of metals. (a) Residual resistivity (ρ_0) vs $T^* = A_1/A_2$. Bad metals, recognized by their large ρ_0, are shown to display the largest A_2 and the lowest T^* (the quadratic term dominates the scattering in the widest temperature range), while in strange metals (encircled in orange in all the figures) it is the linear term that dominates at most temperatures. (b) ρ_0 vs A_2, representing the magnitude of coherent contributions to the electron scattering rate.

characterized by a large ρ_0; the rest of the metals (mostly correlated electron systems) display intermediate values of ρ_0 and some of them show a large T^* [see Fig. 4(a)]. These are the strange metals. We have mentioned the difficulties in the classification of some systems such as Sr_2RuO_4, CrO_2, or $NdNiO_3$. Our analysis suggest that these materials may be classified as belonging to the intermediate A_2 regime of correlated materials and are quite far from the values of bad and good metals [see Fig. 4(b)]. Interestingly, these three materials happen to be unexpectedly clean, according to the ρ_0 obtained from the DC-PRF analysis, which are comparable to those of the simple metals, as shown in Fig. 3(d). This observation is an example of the potential benefit of the present proposal to provide a consistent classification of metallic transport on the basis of these two simple parameters.

It is also worth noticing that, in those cases in which $A_2 \ll A_1$, the description of $\rho_{\text{ideal}}(T)$ with a linear and quadratic term is a very good approximation to the actual data, while larger A_2 values, approaching A_1, indicate that adding higher-order terms in the Taylor expansion is needed in order to better reproduce the data. We have done that in the case of $Bi_2Sr_2Ca_{0.89}Y_{0.11}Cu_2O_y$ (Fig. S35 in the Supplemental Material [38]), Rb_3C_{60} (Fig. S36 in the Supplemental Material), and $YBa_2Cu_3O_{6.45}$ (Fig. S37 in the Supplemental Material), showing that this indeed gives better fits. Both the residual resistivity and the linear coefficient are kept unchanged with respect to the original fit. The addition of a higher-order term reduces both A_2 and ρ_{sat}, emphasizing the phenomenological character of these values, and showing that A_2 in Fig. 3 encompasses the nonlinear contributions to the scattering rate.

III. CONCLUSION

The customary classification of metals as normal, bad, or strange runs short to describe the complexity of electron correlated systems, often leading to controversial conclusions. We show that the Hussey formalism applied to cuprates, which consist of T-linear (A_1) and T-quadratic (A_2) components added to the residual resistivity and in parallel with a saturation term, can describe the behavior of metals far more generally, offering the opportunity for a unified description. Moreover, we also showed that defining a temperature $T^* = A_1/A_2$ may provide a general framework to classify metals in accordance with the relative magnitude of ρ_0 and T^*. In strange metals, T^* describes the crossover from coherent quasiparticle scattering to scale-invariant "Planckian" dissipation. Generally, A_1 and A_2 do not have a well-defined physical origin and they simply represent the incoherent dissipation and the coherent quasiparticle scattering contributions to the resistivity, respectively. A_1 is found to reach an upper bound, for sufficiently large (m^*/n) ratios. The clear link of this bound with the Planckian dissipation limit supports its proposed universality [9,33], extending its scope to a larger number of metals and evidencing that all metals may obey the Planckian constrain.

The data that support the findings of this study are openly available at the following Ref. [46].

ACKNOWLEDGMENTS

We are indebted to N. Hussey, J. Zaanen, T. Palstra, and F. Rivadulla for insightful discussions. We are grateful to J. Baas, A. Joshua, and H. Bonder for their invaluable technical support. Q.G. acknowledges financial support from a China Scholarship Council (CSC) grant and Q.G. and B.N. acknowledge financial support from CogniGron and the Ubbo Emmius Funds (University of Groningen).

Q.G. and B.N. designed the project; Q.G. synthesized the nickelate films and performed the transport measurements. C.M. performed the electron microscopy measurements and analyzed the data. Q.G. collected all the reported data and performed the fits and analysis with feedback from all the authors. Q.G. and B.N. wrote the first version of the manuscript. All the authors discussed the results, and read and contributed to the different versions of the manuscript.

The authors declare no competing financial or nonfinancial interests.

[1] L. D. Landau, Sov. Phys. JETP **8**, 70 (1959).
[2] G. R. Stewart, Rev. Mod. Phys. **73**, 797 (2001).
[3] S.-S. Lee, Annu. Rev. Condens. Matter Phys. **9**, 227 (2018).
[4] A. F. Ioffe and A. R. Regel, Prog. Semicond. **4**, 237 (1960).

[5] The Mott-Ioffe-Regel (MIR) limit reflects the electrons' mean free path approaching the interatomic spacing.

[6] O. Gunnarsson, M. Calandra, and J. E. Han, Rev. Mod. Phys. **75**, 1085 (2003).

[7] N. E. Hussey, K. Takenaka, and H. Takagi, Philos. Mag. **84**, 2847 (2004).

[8] K. Takenaka, R. Shiozaki, S. Okuyama, J. Nohara, A. Osuka, Y. Takayanagi, and S. Sugai, Phys. Rev. B **65**, 092405 (2002).

[9] J. Bruin, H. Sakai, R. S. Perry, and A. P. Mackenzie, Science **339**, 804 (2013).

[10] P. B. Allen, T. P. Beaulac, F. S. Khan, W. H. Butler, F. J. Pinski, and J. C. Swihart, Phys. Rev. B **34**, 4331 (1986).

[11] G. W. Crabtree, D. H. Dye, D. P. Karim, S. A. Campbell, and J. B. Ketterson, Phys. Rev. B **35**, 1728 (1987).

[12] N. W. Ashcroft and N. D. Mermin, *Solid State Physics* (Saunders College Publishing, Philadelphia, 1976).

[13] J. W. C. De Vries, Thin Solid Films **167**, 25 (1988).

[14] A. Eiling and J. Schilling, J. Phys. F **11**, 623 (1981).

[15] R. Cooper, Y. Wang, B. Vignolle, O. J. Lipscombe, S. Hayden, Y. Tanabe, T. Adachi, Y. Koike, M. Nohara, H. Takagi *et al.*, Science **323**, 603 (2009).

[16] H. Takagi, B. Batlogg, H. L. Kao, J. Kwo, R. J. Cava, J. J. Krajewski, and W. F. Peck, Jr., Phys. Rev. Lett. **69**, 2975 (1992).

[17] W. J. Padilla, Y. S. Lee, M. Dumm, G. Blumberg, S. Ono, K. Segawa, S. Komiya, Y. Ando, and D. N. Basov, Phys. Rev. B **72**, 060511(R) (2005).

[18] N. L. Wang, C. Geibel, and F. Steglich, Physica C **262**, 231 (1996).

[19] A. F. Hebard, T. T. M. Palstra, R. C. Haddon, and R. M. Fleming, Phys. Rev. B **48**, 9945 (1993).

[20] D. Varshney, High Press. Res. **26**, 203 (2006).

[21] T. Ito, K. Takenaka, and S.-I. Uchida, Phys. Rev. Lett. **70**, 3995 (1993).

[22] A. W. Tyler, A. P. Mackenzie, S. Nishizaki, and Y. Maeno, Phys. Rev. B **58**, R10107 (1998).

[23] M. J. Besnus, J. P. Kappler, P. Lehmann, and A. Meyer, Solid State Commun. **55**, 779 (1985).

[24] J. Flouquet, S. Kambe, L. P. Regnault, P. Haen, J. P. Brison, F. Lapierre, and P. Lejay, Phys. B: Condens. Matter **215**, 77 (1995).

[25] S. P. Lewis, P. B. Allen, and T. Sasaki, Phys. Rev. B **55**, 10253 (1997).

[26] K. Suzuki and P. M. Tedrow, Phys. Rev. B **58**, 11597 (1998).

[27] L. Ranno, A. Barry, and J. M. D. Coey, J. Appl. Phys. **81**, 5774 (1997).

[28] H. Y. Hwang and S.-W. Cheong, Science **278**, 1607 (1997).

[29] P. B. Allen, R. M. Wentzcovitch, W. W. Schulz, and P. C. Canfield, Phys. Rev. B **48**, 4359 (1993).

[30] Z. Fisk and G. W. Webb, Phys. Rev. Lett. **36**, 1084 (1976).

[31] R. Jaramillo, S. D. Ha, D. Silevitch, and S. Ramanathan, Nat. Phys. **10**, 304 (2014).

[32] D. Li, B. Y. Wang, K. Lee, S. P. Harvey, M. Osada, B. H. Goodge, L. F. Kourkoutis, and H. Y. Hwang, Phys. Rev. Lett. **125**, 027001 (2020).

[33] A. Legros, S. Benhabib, W. Tabis, F. Laliberté, M. Dion, M. Lizaire, B. Vignolle, D. Vignolles, H. Raffy, Z. Li *et al.*, Nat. Phys. **15**, 142 (2019).

[34] Y. Nakajima, T. Metz, C. Eckberg, K. Kirshenbaum, A. Hughes, R. Wang, L. Wang, S. R. Saha, I.-L. Liu, N. P. Butch *et al.*, Commun. Phys. **3**, 181 (2020).

[35] N. E. Hussey, R. A. Cooper, X. Xu, Y. Wang, I. Mouzopoulou, B. Vignolle, and C. Proust, Philos. Trans. R. Soc. A **369**, 1626 (2011).

[36] H. Wiesmann, M. Gurvitch, H. Lutz, A. Ghosh, B. Schwarz, M. Strongin, P. B. Allen, and J. W. Halley, Phys. Rev. Lett. **38**, 782 (1977).

[37] N. E. Hussey, J. Phys.: Condens. Matter **20**, 123201 (2008).

[38] See Supplemental Material at http://link.aps.org/supplemental/10.1103/PhysRevB.106.085141 for information on the characterization of thin films, the fit to resistivity data of various metallic systems, relevant parameters for different metals, analysis of Taylor expansion, and determination of errors.

[39] D. Li, K. Lee, B. Y. Wang, M. Osada, S. Crossley, H. R. Lee, Y. Cui, Y. Hikita, and H. Y. Hwang, Nature (London) **572**, 624 (2019).

[40] E. Mikheev, A. J. Hauser, B. Himmetoglu, N. E. Moreno, A. Janotti, C. G. Van de Walle, and S. Stemmer, Sci. Adv. **1**, e1500797 (2015).

[41] J. Liu, M. Kargarian, M. Kareev, B. Gray, P. J. Ryan, A. Cruz, N. Tahir, Y.-D. Chuang, J. Guo, J. M. Rondinelli *et al.*, Nat. Commun. **4**, 2714 (2013).

[42] Q. Guo, S. Farokhipoor, C. Magén, F. Rivadulla, and B. Noheda, Nat. Commun. **11**, 2949 (2020).

[43] Q. Guo and B. Noheda, npj Quantum Mater. **6**, 72 (2021).

[44] C. H. Mousatov and S. A. Hartnoll, npj Quantum Mater. **6**, 81 (2021).

[45] Bear in mind that correlation is not causation, since it is easy to get an ordinary metal with a high ρ_0.

[46] The parameters resulting from all the fits and their errors can be found at https://doi.org/10.34894/A1AHZR.

[47] N. R. Poniatowski, T. Sarkar, S. DasSarma, and R. L. Greene, Phys. Rev. B **103**, L020501 (2021).

[48] In a more detailed analysis, this definition could be extended to T^*/W, where W is the bandwidth of the bands crossing the Fermi energy, so as to obtain an adimensional figure of merit to assess the relative relevance of scattering mechanisms.

[49] J. Ayres, M. Berben, M. Čulo, Y.-T. Hsu, E. van Heumen, Y. Huang, J. Zaanen, T. Kondo, T. Takeuchi, J. Cooper *et al.*, Nature (London) **595**, 661 (2021).